0013-7227/03/$15.00/0
Printed in U.S.A.

Endocrinology 144(4):1226–1233

doi: 10.1210/en.2002-220821

Parathyroid Hormone Enhances Mechanically Induced Bone Formation, Possibly Involving L-Type Voltage-Sensitive Calcium Channels

JILIANG LI, RANDALL L. DUNCAN, DAVID B. BURR, VINCENT H. GATTONE, AND CHARLES H. TURNER

Departments of Orthopedic Surgery (J.L., R.L.D., D.B.B., C.H.T.) and Anatomy and Cell Biology (J.L., D.B.B., V.H.G.), Indiana University School of Medicine, Indianapolis, Indiana 46202

PTH and mechanical loading might act synergistically on bone formation. We tested the *in vivo* effect of the L-type voltage-sensitive calcium channel (VSCC) blocker, verapamil, on bone formation induced by human PTH-(1–34) (PTH) injection with or without mechanical loading. Adult rats were divided into eight groups: vehicle, verapamil, PTH, or verapamil plus PTH with or without mechanical loading. Verapamil (100 mg/kg) was given orally 90 min before loading. PTH (80 μg/kg) was injected sc 30 min before loading. Loading applied to tibia and ulna for 3 min significantly increased the bone formation rate on both the endocortical surface of tibia and the periosteal surface of ulna ($P < 0.0001$). Treatment with PTH enhanced load-induced bone formation by 53% and 76% ($P < 0.001$) on the endocortical and periosteal surfaces, respectively. Treatment with verapamil suppressed load-induced bone formation rate by 77% and 59% ($P < 0.01$). Furthermore, verapamil suppressed bone formation in rats subjected to PTH plus loading by 74% and 68% ($P < 0.0001$) at the tibia and ulna, respectively. In the groups without loading, neither verapamil nor PTH treatment significantly changed any bone formation parameter. This study indicates that L-type VSCCs mediate load-induced bone formation *in vivo*. Furthermore, PTH enhances load-induced bone adaptation through involvement of L-type VSCCs. (*Endocrinology* 144: 1226–1233, 2003)

INTERMITTENT administration of the human (h) PTH fragment, hPTH-(1–34) (PTH), stimulates bone formation (1–4). Mechanical loading in combination with PTH treatment has synergistic action on bone formation in rats (5–7). PTH and mechanical loading produce similar responses in osteoblasts, suggesting that one way PTH elicits an anabolic response in bone is by enhancing responsiveness to mechanical loading. An early response to both stimuli is a rapid increase in intracellular calcium ($[Ca^{2+}]_i$) that is dependent on both extracellular Ca^{2+} entry and $[Ca^{2+}]_i$ release (8–10). The early increase in $[Ca^{2+}]_i$ has been linked to increased production of nitric oxide and prostaglandins in osteoblasts (11, 12) and up-regulation of some skeletal growth factors, including IGF-I and TGFβ (13, 14). Both nitric oxide and prostaglandins have been shown to mediate load-induced bone formation *in vivo* (15–17).

Recent cell culture studies show that PTH enhances the intracellular calcium concentration in osteoblastic cells subjected to fluid shear stress, and that the synergistic effect between PTH and fluid shear is attenuated by L-type calcium channel blockers, such as nifedipine (18, 19). These data suggest that PTH enhances fluid shear-induced calcium signaling in osteoblastic cells through activation of L-type voltage-sensitive calcium channels (VSCCs). We hypothesized that PTH affects load-induced bone formation *in vivo* via L-type VSCCs.

We have previously shown that two L-type calcium channel blockers, nifedipine and verapamil, suppress load-induced bone formation in rats (20), suggesting that L-type VSCCs play a critical role in mechanically induced bone formation *in vivo*. In the present study we tested the *in vivo* effect of the L-type VSCC blocker, verapamil, on bone formation after PTH injection and/or mechanical loading.

Abbreviations: BFR/BS, Bone formation rate/bone surface; $[Ca^{2+}]_i$, intracellular calcium; h, human; MAR, mineral apposition rate; MS/BS, mineralizing surface/bone surface; PLSD, protected least significant difference; r, relative; VSCC, voltage-sensitive calcium channel.

Materials and Methods

Experimental animals

A total of 64 adult female Sprague Dawley rats were used for this study. The rats were housed one per cage at the Laboratory Animal Resource Center of Indiana University School of Medicine and were fed standard rat chow and water *ad libitum*. The animals were allowed to acclimate for 2 wk before the experiment began and were approximately 7 months old at the beginning of the study. All procedures performed in this study were in accordance with the Indiana University animal care and use committee guidelines.

Experimental design

The rats were randomly divided into eight groups (n = 8/group): 1) vehicle treated; 2) verapamil treated; 3) PTH treated; 4) verapamil plus PTH treated; 5) vehicle plus mechanical loading; 6) verapamil plus loading; 7) PTH plus loading; and 8) verapamil, PTH, and loading (Fig. 1). For the groups without loading, one group was given vehicle treatment only. The other three groups were given verapamil orally (100 mg/kg; Sigma-Aldrich, St. Louis, MO) and/or hPTH-(1–34) sc (80 μg/kg; Bachem California, Inc., Torrance, CA) or both verapamil and PTH. The same treatments were given to the remaining four groups with loading. Verapamil and hPTH-(1–34) were given 90 and 30–40 min before loading, respectively. The doses and dosing regimens were selected based on the previous studies (5, 20).

Verapamil was dissolved in polyethylene glycol 400 (Sigma-Aldrich) to form a 10-mg/ml solution (21), stirred overnight, wrapped in aluminum foil to protect the solution from light, and stored at room temperature. The vehicle consisted of polyethylene glycol 400. The drug was

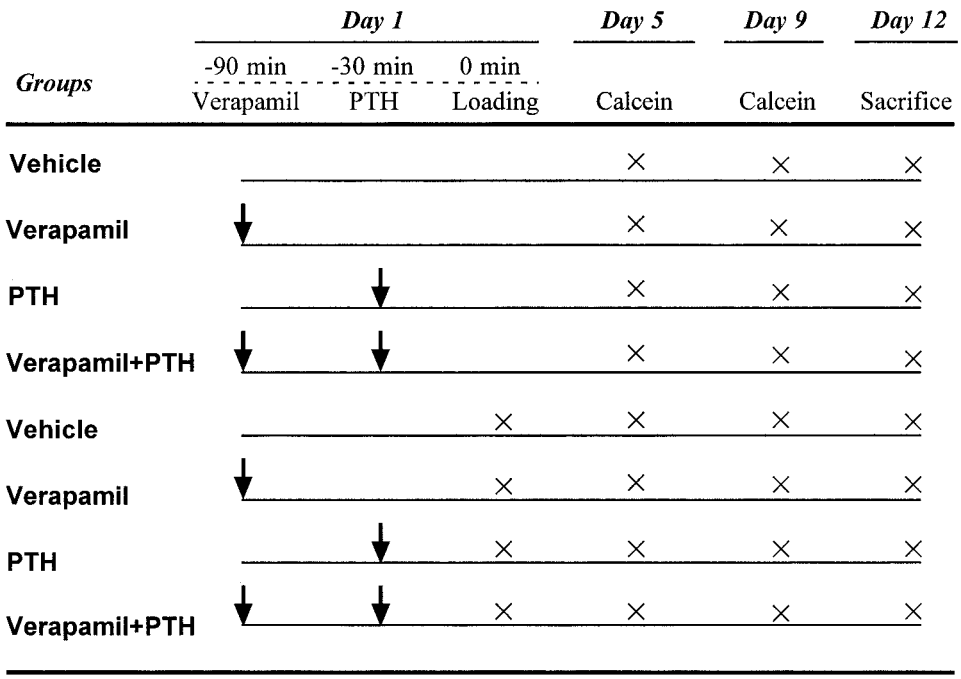

FIG. 1. Overview of the experimental design. Rats were equally divided into eight groups. Half of the animals were treated with vehicle, verapamil, PTH, or verapamil plus PTH without loading, The other half received the various drug treatments and mechanical loading of the ulna and tibia. Verapamil was given 90 min before, and PTH was given 30 min before loading. All animals were labeled with injection of calcein on d 5 and 9, and were killed on d 12.

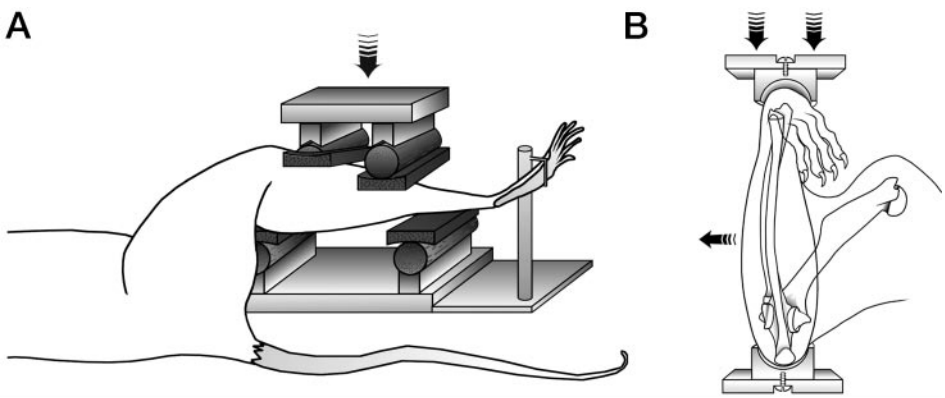

FIG. 2. A, Diagram of the rat tibia four-point bending system. The right tibia is fixed between two upper load points (11 mm apart) and two supports (23 mm apart). When force is applied, a mediolateral bending moment is produced in the central portion of the tibial shaft. This figure is reprinted from the report by Robling *et al.* (54) with permission from the publisher. B, Schematic diagram of the rat ulna loading model. The right forearm is held between upper and lower cups. The force (*upper large arrows*) is applied through the carpal joint and overlying soft tissues. Axial load is translated into a bending moment (*small arrow*) in the ulnar diaphysis due to preexisting mediolateral curvature. This figure is reprinted from the report by Robling *et al.* (55) with permission from the publisher.

administered to the rats by gavage. Oral administration of verapamil causes a peak plasma level 90 min later, coincident with loading (22). The hormone vehicle for hPTH-(1–34) was acidified saline containing 2% heat-inactivated rat sera (1). A single sc injection of hPTH-(1–34) leads to peak serum concentration at 30–60 min after administration in rats, also coincident with loading (5, 23). Normal PTH levels are restored within 4 h, and a single sc injection of PTH has no significant effect on plasma calcium levels (22). Rats from the loaded groups were subjected to four-point bending of the right tibia and axial loading of the right ulna.

Loading protocol

A single bout of mechanical loading was applied as a haversine wave with a frequency of 2 Hz and a duration of 3 min (360 cycles) to both right ulna and right tibia. For tibial bending, force was applied through a four-point bending apparatus (Fig. 2A) using a load-controlled, electromagnetic loading device (24). The peak load on the tibia was 63 N. The peak compressive strains at the tibiae midshaft were approximately 3000 $\mu\epsilon$ on the lateral periosteal surface and 1700 $\mu\epsilon$ on the lateral endocortical surface (25). For axial loading on the ulna, force was applied across the flexed carpus and olecanon as described by Torrance *et al.* (26) (Fig. 2B) using a stepper motor-driven spring linkage. The peak load on the ulna was 16.5 N, resulting in a peak compressive strain of 3600 $\mu\epsilon$ on the medial surface of the ulnar midshaft (27). We chose loading protocols that would induce a similar level of new bone formation in the tibia (endocortical surface) and ulna (periosteal surface).

Before the loading session, rats were anesthetized with an ip injection of a mixed solution of ketamine hydrochloride (50 mg/kg; Fort Dodge Animal Health, Fort Dodge, IA) and xylazine (10 mg/kg; The Butler Co.,

Columbus, OH). After loading bouts, rats were allowed normal cage activity.

Bone labeling, processing, and histomorphometry

All rats were given an ip injection of a fluorochrome bone label (7 mg/kg calcein; Sigma-Aldrich) on d 4 and 9 after loading and were killed 3 d after the second label. The calcein label was administered 4 d after loading because previous experiments have shown that bone formation is initiated 96 h after mechanical loading (28). The right and left tibiae and ulnae were removed, cleaned of soft tissue, and cleaved at the distal and proximal ends to allow proper infiltration of plastic into the marrow cavity. Specimens were immersed in 10% neutral buffered formalin for 48 h to fix the tissues. The specimens were then dehydrated in graded alcohols, cleared in xylene, and embedded in methyl methacrylate. Using a diamond-embedded wire saw (Histo-saw, Delaware Diamond Knives, Wilmington, DE), three transverse thick sections (~70 μm) were cut from the tibial diaphyses 4–8 mm proximal to the tibia-fibula junction (this region is under maximal bending during four-point loading) and from ulna diaphysis 2–3 mm distal to the ulnar midpoint, which has been shown to be most responsive to loading (29), and mounted unstained on standard microscope slides.

One slide per limb was read on an Optiphot fluorescence microscope (Nikon, Garden City, NY). Using the Bioquant digitizing system (R&M Biometrics, Nashville, TN), the following primary data were collected, respectively, from the endocortical surface of tibiae and from periosteal surfaces of ulnae at ×150 magnification: bone perimeter (B.Pm), single label perimeter (sL.Pm), double label perimeter (dL.Pm), and double label area (dL.Ar). From these primary data, the following calculations were performed: mineralizing surface [MS/bone surface (BS) = (1/2 sL.Pm + dL.Pm/B.Pm); percentage], mineral apposition rate (MAR = dL.Ar/dl.Pm·4 d; microns per day), lamellar bone formation rate (BFR/BS = MAR × MS/BS × 3.65; cubic microns per square microns per year). To examine mechanically induced bone formation, bone formation parameters from the left limb (nonloaded control) were subtracted from right limb values, producing a new set of relative values for each variable: rMS/BS, rMAR, and rBFR/BS.

Effects of verapamil on blood pressure, serum PTH, and serum calcium

In this study the dose of verapamil administered to rats was much higher than that used in clinical applications. High doses of verapamil may cause hypotension (22) or increase PTH secretion (30, 31), which, in turn, might change the serum calcium level. We looked into these possibilities by conducting a separate experiment to study the effect of a single high dose verapamil treatment (100 mg/kg, orally) on blood pressure, serum PTH, and serum calcium in rats.

Blood pressure was measured in five rats before, 45 min after, and 90 min after a single treatment with verapamil (100 mg/kg). Systolic blood pressure (mm Hg) was measured indirectly using a tail-cuff blood pressure system (model 129, IITC Life Sciences, Woodland Hills, CA). Rats were restrained in holders and placed within a chamber maintained at 27 C. A tail cuff with photoelectric detector was placed at the base of the tail and inflated. As the cuff pressure was slowly released, the photoelectric cell detected the initiation of arterial blood flow through the tail artery, which was recorded as the systolic blood pressure. Several measurements were taken at each time point and averaged.

Blood samples were collected from five untreated rats, five verapamil-treated rats at 45 min after a dose of verapamil, and 90 min after a dose of verapamil (100 mg/kg). Blood samples were allowed to clot at room temperature and then were centrifuged at 2000 rpm for 15 min. Sera were separated from those blood samples for measurements of serum PTH and serum calcium. Serum PTH (picograms per milliliter) was measured using a rat PTH immunoradiometric assay kit (Immunotopics, San Clemente, CA). Serum calcium (milligrams per deciliter) was measured using a Roche Cobas Mira Analyzer (GMI, Inc., Albertville, MN).

Statistical analysis

The data are expressed as the mean ± SEM. Bartlett's test (a test of the homogeneity of variances among groups) indicated that group variances were equal ($P > 0.5$), suggesting that parametric statistical tests were valid. Differences between the loaded (right) and nonloaded (left) limbs were tested using paired t tests. Differences among group means were tested for significance by ANOVA, followed by Fisher's protected least

TABLE 1. Measurements of endocortical bone formation at tibia

Groups	Load	n	MAR (μm/d)		MS/BS (%)		BFR/BS ($\mu m^3/\mu m^2$·yr)	
			Mean ± SEM	P value[a]	Mean ± SEM	P value[a]	Mean ± SEM	P value[a]
Vehicle								
Right	N	8	0.63 ± 0.09	N.S.	26.74 ± 4.84	N.S.	70.30 ± 16.15	N.S.
Left		8	0.67 ± 0.08		24.27 ± 3.57		65.41 ± 13.39	
Verapamil								
Right	N	8	0.59 ± 0.07	N.S.	29.34 ± 3.89	N.S.	68.32 ± 12.08	N.S.
Left		8	0.57 ± 0.06		26.87 ± 4.60		60.05 ± 10.94	
PTH								
Right	N	8	0.66 ± 0.05	N.S.	28.82 ± 2.92	N.S.	70.96 ± 10.73	N.S.
Left		8	0.62 ± 0.05		25.26 ± 3.37		59.34 ± 11.36	
Verapamil + PTH								
Right	N	8	0.65 ± 0.04	N.S.	30.60 ± 4.13	N.S.	76.70 ± 14.47	N.S.
Left		8	0.66 ± 0.05		25.58 ± 4.27		65.11 ± 14.56	
Vehicle								
Right	Y	8	0.91 ± 0.07	<0.01	46.28 ± 3.88	<0.001	155.98 ± 18.93	<0.001
Left		8	0.73 ± 0.07		23.19 ± 2.90		64.65 ± 12.51	
Verapamil								
Right	Y	8	0.78 ± 0.06	<0.05	28.64 ± 2.82	<0.001	82.00 ± 10.97	<0.01
Left		8	0.70 ± 0.08		22.90 ± 2.93		60.89 ± 11.21	
PTH								
Right	Y	8	1.00 ± 0.11	<0.05	55.69 ± 3.93	<0.001	204.25 ± 27.69	<0.001
Left		8	0.72 ± 0.04		24.40 ± 2.65		64.25 ± 6.68	
Verapamil + PTH								
Right	Y	8	0.84 ± 0.07	<0.05	35.00 ± 5.26	<0.05	110.42 ± 21.69	<0.01
Left		8	0.70 ± 0.06		27.52 ± 3.97		73.56 ± 15.46	

Values are means ± SEM; N, No; Y, yes.

[a] Probability associated with paired t test between right and left values for each group. N.S. (not significant) indicates that the probability exceeds 0.05.

significant difference test (PLSD) for pairwise comparisons. Statistical significance was assumed if $P < 0.05$.

Results

There were no differences in body weight among the groups at the beginning or end of the experimental period. The treatment with verapamil did not affect the animals' activities throughout the experiment. Compared with the baseline blood pressure (118.8 ± 2.04 mm Hg), the average blood pressure decreased by 4% and 12% at 45 min (113 ± 2.07 mm Hg) and 90 min (104.6 ± 6.75 mm Hg) after treatment with verapamil, respectively, but the changes were not statistically significant. Compared with the normal total serum calcium (10.20 ± 0.07 mg/dl), serum calcium was significantly increased to 11.2 ± 0.22 mg/dl 45 min after verapamil treatment, but returned to normal levels (10.18 ± 0.17 mg/dl) 90 min after treatment. There were no significant differences in serum PTH among the normal controls (12.38 ± 2.64 pg/ml) and animals 45 min after (10.13 ± 2.43 pg/ml) and 90 min after (11.18 ± 3.92 pg/ml) a single dose of verapamil.

Bone formation on the endocortical surface of tibiae

Histomorphometric measurements show that there was no significant difference in MS/BS, MAR, and BFR/BS between right and left tibiae in the groups without loading, as analyzed by the paired *t* tests (Table 1). However, in the loading control group there were significantly higher MS/BS, MAR, and BFR/BS in loaded (right) tibiae ($P < 0.01$) compared with nonloaded (left) tibiae. Significant differences in MS/BS, MAR, and BFR/BS between right and left tibiae were also found for all loading groups regardless of treatment ($P < 0.05$; Table 1). The values for MS/BS, MAR, and BFR/BS of left tibiae were not significantly different among the groups. Treatment with verapamil significantly reduced the mechanical loading effects on bone. Verapamil suppressed the load-induced increase in MS/BS and BFR/BS by 75% ($P < 0.05$) and 77% ($P < 0.001$), respectively (Fig. 3). In contrast, PTH significantly enhanced the load-induced increase in MS/BS and BFR/BS by 36% ($P < 0.05$) and 53% ($P < 0.01$), respectively. Verapamil suppressed rMS/BS and rBFR/BS on the right loaded tibiae in the animals subjected to PTH and loading by 76% ($P < 0.001$) and 74% ($P < 0.0001$), respectively.

Bone formation on the periosteal surface of ulnae

Histomorphometric measurements showed that there was no significant difference in MS/BS, MAR, and BFR/BS between right and left ulnae in the groups without loading (Table 2). However, there were significantly higher MS/BS, MAR, and BFR/BS in loaded (right) ulnae of the loading control animals ($P < 0.01$) compared with nonloaded (left) ulnae. Significant differences in MS/BS, MAR, and BFR/BS between right and left ulnae were also found for all treatment groups with loading ($P < 0.05$; Table 2). The values for MS/BS, MAR, and BFR/BS of left (nonleaded) ulnae were not significantly different among the groups. Similar to that in tibia, treatment with verapamil significantly inhibited the mechanical loading effects on right loaded ulnae. Verapamil

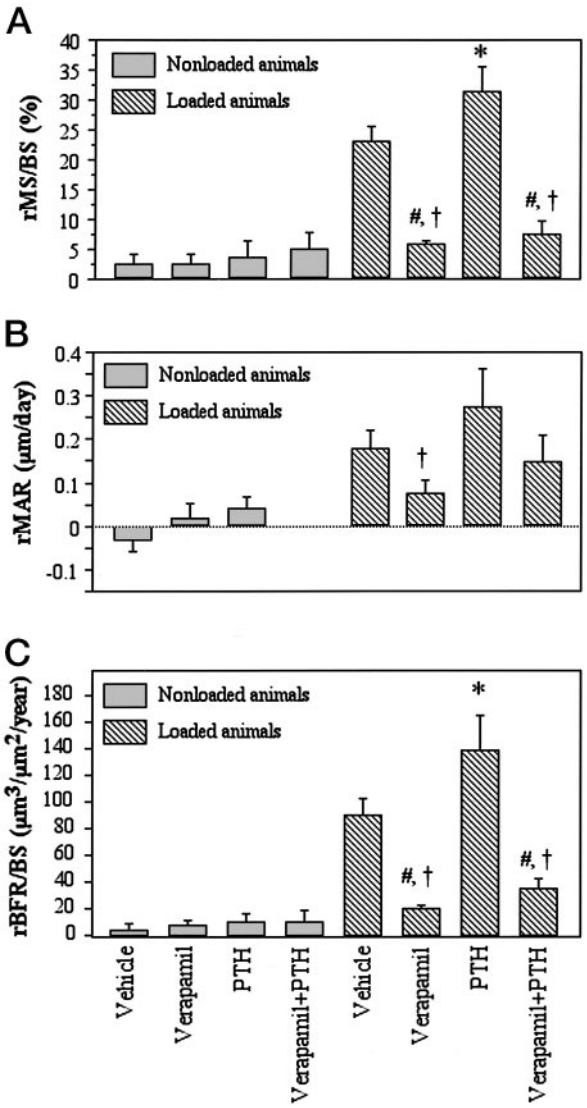

FIG. 3. On the endocortical surface of tibia, the rMS/BS (A) and rBFR/BS (B) were significantly decreased by verapamil. PTH plus loading led to significantly higher rBFR/BS and rMS/BS than the loading alone. Verapamil suppressed the synergistic effect of PTH and loading. There was a significant difference in the rMAR (B) between verapamil treatment and PTH treatment in loaded animals. Results are expressed as the mean ± SEM. *, $P < 0.05$ *vs.* vehicle loading group; #, $P < 0.001$ *vs.* vehicle loading group; †, $P < 0.05$ *vs.* PTH loading group (based on Fisher's PLSD at $\alpha = 0.05$).

suppressed the load-induced increase in MS/BS and BFR/BS in the loading controls by 22% ($P = 0.056$) and 59% ($P < 0.01$), respectively (Fig. 4). PTH significantly enhanced the loading effect on the right loaded ulnae, increasing rMS/BS by 63% ($P < 0.01$) and rBFR/BS by 76% ($P < 0.01$). Furthermore, verapamil suppressed rMS/BS and rBFR/BS on right loaded ulnae in animals subjected to PTH and loading by 39% ($P < 0.01$) and 68% ($P < 0.001$), respectively.

Discussion

We studied the *in vivo* effect of PTH on load-induced bone formation in a system in which the L-type VSCCs were blocked by verapamil. The mechanical loading was carried

TABLE 2. Measurements of periosteal bone formation at ulna

Groups	Load	n	MAR (μm/d)		MS/BS (%)		BFR/BS ($\mu m^3/\mu m^2 \cdot yr$)	
			Mean ± SEM	*P* value[a]	Mean ± SEM	*P* value[a]	Mean ± SEM	*P* value[a]
Vehicle								
Right	N	8	0.66 ± 0.04	N.S.	37.66 ± 4.04	N.S.	91.86 ± 12.10	N.S.
Left		8	0.68 ± 0.05		33.24 ± 3.26		82.62 ± 9.65	
Verapamil								
Right	N	8	0.67 ± 0.06	N.S.	34.38 ± 1.02	N.S.	84.10 ± 6.83	N.S.
Left		8	0.68 ± 0.04		31.76 ± 1.31		79.83 ± 8.02	
PTH								
Right	N	8	0.72 ± 0.06	N.S.	36.19 ± 3.18	N.S.	98.08 ± 14.25	N.S.
Left		8	0.70 ± 0.05		32.42 ± 3.42		85.48 ± 12.76	
Verapamil + PTH								
Right	N	8	0.66 ± 0.04	N.S.	37.02 ± 2.35	N.S.	90.95 ± 11.62	N.S.
Left		8	0.64 ± 0.03		32.10 ± 1.72		74.62 ± 3.47	
Vehicle								
Right	Y	8	1.11 ± 0.10	<0.01	59.73 ± 2.54	<0.001	239.43 ± 19.91	<0.001
Left		8	0.71 ± 0.02		37.70 ± 1.45		97.92 ± 5.42	
Verapamil								
Right	Y	8	0.83 ± 0.06	<0.01	49.34 ± 3.06	<0.05	149.71 ± 14.08	<0.01
Left		8	0.57 ± 0.02		36.95 ± 2.62		91.22 ± 11.80	
PTH								
Right	Y	8	1.31 ± 0.11	<0.01	71.66 ± 2.49	<0.001	345.88 ± 37.96	<0.001
Left		8	0.75 ± 0.02		35.67 ± 2.81		97.07 ± 7.51	
Verapamil + PTH								
Right	Y	8	0.80 ± 0.08	N.S.	55.39 ± 5.07	<0.01	165.78 ± 25.13	<0.05
Left		8	0.70 ± 0.06		33.49 ± 3.22		85.52 ± 12.25	

Values are means ± SEM; N, No; Y, yes.

[a] Probability associated with paired *t* test between right and left values for each group. N.S. (not significant) indicates that the probability exceeds 0.05.

out using established *in vivo* loading models: rat tibial four-point bending and ulna axial loading (16, 17, 20). Similar to previous studies (16, 17, 20), a single bout of four-point bending was sufficient to significantly increase lamellar bone formation on the endocortical surface of the tibia, and a single bout of axial loading was sufficient to significantly increase lamellar bone formation on the periosteal surface of the ulna. As we have reported previously (20), a single verapamil treatment significantly inhibited load-induced bone formation compared with that in the loading control group. Consistent with a previous report (5), a single PTH treatment significantly enhanced load-induced bone formation compared with loading alone. Moreover, verapamil treatment significantly suppressed bone formation in animals subjected to PTH treatment and loading.

We conclude that the synergism between PTH and mechanical loading in their effect on bone formation is mediated in part by Ca^{2+} entry into the osteoblast through L-type VSCCs. This conclusion is supported by *in vitro* experiments showing that PTH pretreatment of osteoblasts before mechanical loading produces a greater peak $[Ca^{2+}]_i$ response than loading alone (18, 32, 33) and the observation that PTH can modulate VSCC-mediated Ca^{2+} influx and at least partially amplify L-type VSCC currents in various cell models (19, 34–38). In addition, PTH can increase the activity and single channel conductance of the mechanically sensitive, cation-selective channel in UMR106.01 osteoblast-like cells (39). Changes in the activation kinetics of the mechanically sensitive channel produce a membrane depolarization that could activate L-type VSCCs.

The earliest response of osteoblasts to fluid shear or mechanical strain is a rapid increase in $[Ca^{2+}]_i$ (8), which can be suppressed by L-type VSCC blockers (33). On the other hand, PTH can enhance shear flow-induced increase in $[Ca^{2+}]_i$ osteoblastic cells, which can also be suppressed by the L-type VSCC blocker nifedipine (19). Furthermore, in osteoblasts, blockade of L-type VSCCs using either verapamil or nifedipine inhibits $[Ca^{2+}]_i$ signals and consequent cellular responses induced by PTH (18, 40–42). The L-type VSCC is the best characterized channel among the voltage-sensitive and voltage-insensitive currents that have been measured in osteoblasts, stromal precursor cells, osteocytes, and osteoblast-like clonal cell lines (for review, see Ref. 43). These channels may play a role in normal bone physiology. Low doses of nifedipine given to growing rabbits over 10 wk significantly reduce cancellous and cortical bone volume, MAR, and the length of the epiphyseal growth plate (44).

Intermittent administration of PTH increases bone mass and improves bone structure *in vivo* (1–3). Osteoblasts are the primary target cells for the anabolic effects of PTH on bone tissue. PTH may stimulate differentiation of osteoprogenitors (1, 45, 46) and possibly prolong cell longevity (47). Most actions of PTH-(1–34) on osteoblasts are mediated by the PTH-1 receptor, a G protein-coupled receptor with seven membrane-spanning domains (48). PTH can activate the cAMP/protein kinase A pathway, the inositol lipid/Ca^{2+} (release of intracellular Ca^{2+})/protein kinase C pathway, or both in osteoblast-like cells from rat or human (see review in Ref. 49). Like mechanical loading, PTH can also increase $[Ca^{2+}]_i$ in bone cells by increasing both extracellular Ca^{2+} entry and intracellular Ca^{2+} release. PTH could alter calcium channel kinetics via cAMP or PKC (40, 50), possibly through phosphorylation of sites on the various subunits of the channel protein. We have recently demonstrated that the PTH-

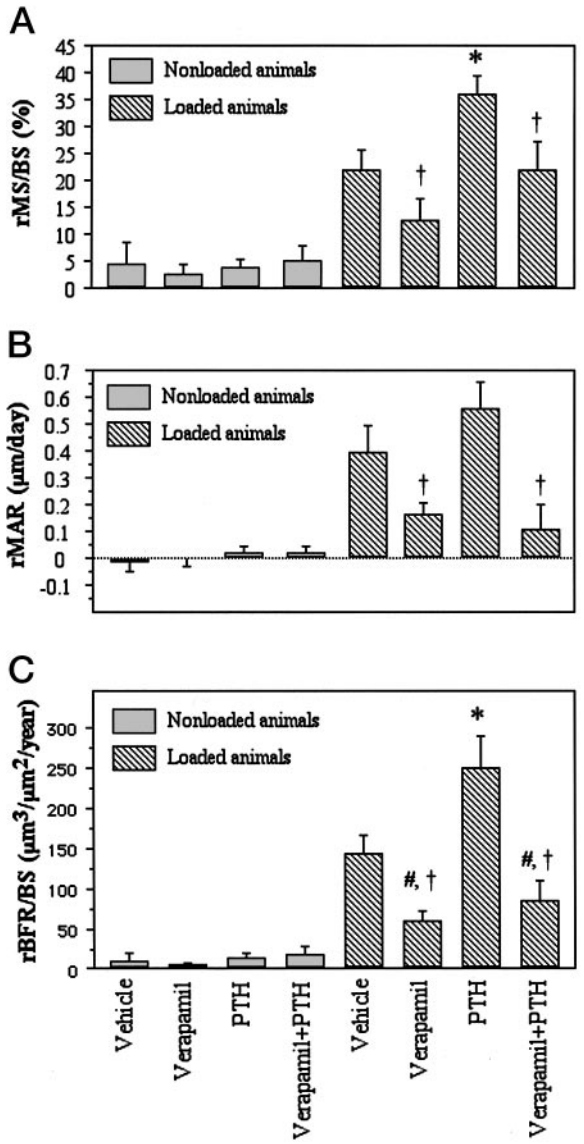

FIG. 4. On the periosteal surface of the ulna, the rMS/BS (A) and rBFR/BS (C) were significantly decreased by verapamil. PTH combined with loading led to significantly higher rBFR/BS and rMS/BS than loading alone. As in the tibia, verapamil suppressed the synergistic effect of PTH and loading. There was a significant difference in the rMAR (B) between verapamil treatment and PTH treatment in loaded animals. The rMAR (B) in animals receiving verapamil, PTH, plus loading was also significantly lower than that in PTH plus loading animals. Results are expressed as the mean ± SEM. *, $P < 0.05$ *vs.* vehicle loading group; #, $P < 0.001$ *vs.* vehicle loading group; †, $P < 0.05$ *vs.* PTH loading group (based on Fisher's PLSD at $\alpha = 0.05$).

enhanced peak $[Ca^{2+}]_i$ response to mechanical stimulation can be blocked by the L-type VSCC inhibitor, nifedipine. Furthermore, this enhanced response could be mimicked through activation of the protein kinase A, but not the protein kinase C, pathway (18).

The dose of verapamil used in the present study was higher than the typical dose (4 mg/kg) used in humans. The goal of clinical use is to partially block L-type VSCCs, reducing their activity in the heart and thus treating arrhythmias. To completely block the L-type VSCC, as we intended in this study, a higher dose was necessary. Verapamil at 100 mg/kg was chosen because of its previously demonstrated lack of toxicity on normal bone formation (20). A high dose of verapamil, 100 mg/kg, did not change blood pressure or serum PTH level. Treatment with 100 mg/kg verapamil also did not significantly affect bone formation in the left (control) bones of the rats in the present study, nor was bone formation affected in the vehicle controls. Our data strongly suggest that 100 mg/kg verapamil given as a single dose does not substantially affect the rats' overall health or skeletal biology.

Even with the high dose of verapamil used in this study, bone formation induced by mechanical loading and by PTH plus mechanical loading was not abolished completely. Administration of verapamil suppressed BFR by 59–77%, which is substantial, yet mechanical loading significantly increased bone formation even in the presence of verapamil. Considering the high dose of verapamil used, it is reasonable to assume that the majority of L-type VSCCs in bone cells were blocked. Consequently, there must be another signaling pathway independent of the L-type VSCC that contributes about 25–40% to the bone formation resulting from mechanical loading or PTH plus loading.

At the 100-mg/kg dose, verapamil might have effects not specific to the L-type VSCC. Previous studies have shown a possible effect of verapamil on PTH secretion (30, 31, 51, 52). In our study, serum PTH did not change after a dose of verapamil, nor was the serum calcium level different from normal at the time of loading. These findings suggest that verapamil treatment did not have substantial side-effects, and the observed effects of treatment were probably due to the effect of verapamil on calcium channels. Verapamil has also been reported to modulate *p*-glycoprotein, a multidrug transporter on cell membrane (53). We cannot rule out this pathway as a mechanism for the verapamil response in the present study. However, we know of no evidence relating *p*-glycoprotein to mechanically induced bone formation. In our previous study we showed that 20 mg/kg of both verapamil and another L-type VSCC blocker, nifedipine, suppressed mechanically induced bone formation. The primary effect of both drugs was on L-type VSCCs, and at the 20-mg/kg dose, few nonspecific effects should be expected (22). Verapamil administered at 100 mg/kg had very similar effects on load-induced bone formation as the 20-mg/kg dose (20), suggesting that the higher dose of verapamil does not activate pathways in addition to the primary effect on L-type VSCCs. Other considerations include the possibility that verapamil alters the vasculature by inducing vasodilation. Our data demonstrate that a single high dose of verapamil lowers blood pressure somewhat, but not significantly. It is possible that altered hemodynamics might affect mechanotransduction in bone tissue by affecting extracellular fluid flow near bone cells. However, as noted above, bone cell mechanotransduction is suppressed by lower doses of verapamil that have much less effect on vascular tone. It seems most likely that the effect of verapamil on bone mechanotransduction was not due to changes in hemodynamics.

In conclusion, the present study suggests that blockade of L-type calcium channels by verapamil suppresses load-induced bone formation on the endocortical surface of tibia and the periosteal surface of ulna. PTH improved load-

induced bone formation in the absence of verapamil, but the improvement was nullified by verapamil. This suggests that PTH enhances mechanically induced bone formation through involvement of L-type calcium channels *in vivo*.

Acknowledgments

We are grateful to Drs. Janet Hock and Jasminka Milas for their advice and help with the preparation of PTH solution. We thank Qiwei Sun, Ming Hu, and Ronald Mcclintock for their help with the measurement of serum PTH and calcium, and Mary Hooser and Diana Jacob for their assistance with tissue processing.

Received August 6, 2002. Accepted December 19, 2002.

Address all correspondence and requests for reprints to: Charles H. Turner, Ph.D., Department of Orthopedic Surgery, Indiana University School of Medicine, 541 Clinical Drive, Suite 600, Indianapolis, Indiana 46202. E-mail: turnerch@iupui.edu.

This work was supported by NIH Grants P01-AR-45218 and R01-DK-58246.

References

1. **Gunness-Hey M, Hock JM** 1984 Increased trabecular bone mass in rats treated with human synthetic parathyroid hormone. Metab Bone Dis Relat Res 5: 177–181
2. **Cosman F, Lindsay R** 1998 Is parathyroid hormone a therapeutic option for osteoporosis? A review of the clinical evidence. Calcif Tissue Int 62:475–480
3. **Jerome CP, Burr DB, Van Bibber T, Hock JM, Brommage R** 2001 Treatment with human parathyroid hormone (1–34) for 18 months increases cancellous bone volume and improves trabecular architecture in ovariectomized cynomolgus monkeys (*Macaca fascicularis*). Bone 28:150–159
4. **Rubin MR, Cosman F, Lindsay R, Bilezikian JP** 2002 The anabolic effects of parathyroid hormone. Osteop Int 13:267–277
5. **Chow JW, Fox S, Jagger CJ, Chambers TJ** 1998 Role for parathyroid hormone in mechanical responsiveness of rat bone. Am J Physiol 274:E146–E154
6. **Hagino H, Okano T, Akhter MP, Enokida M, Teshima R** 2001 Effect of parathyroid hormone on cortical bone response to in vivo external loading of the rat tibia. J Bone Miner Metab 19:244–250
7. **Ma Y, Jee WS, Yuan Z, Wei W, Chen H, Pun S, Liang H, Lin C** 1999 Parathyroid hormone and mechanical usage have a synergistic effect in rat tibial diaphyseal cortical bone. J Bone Miner Res 14:439–448
8. **Hung CT, Allen FD, Pollack SR, Brighton CT** 1996 Intracellular Ca^{2+} stores and extracellular Ca^{2+} are required in the real-time Ca^{2+} response of bone cells experiencing fluid flow. J Biomech 29:1411–1417
9. **Reid IR, Civitelli R, Halstead LR, Avioli LV, Hruska KA** 1987 Parathyroid hormone acutely elevates intracellular calcium in osteoblastlike cells. Am J Physiol 253:E45–E51
10. **Belinsky GS, Morley P, Whitfield JF, Tashjian Jr AH** 1999 Ca^{2+} and extracellular acidification rate responses to parathyroid hormone fragments in rat ROS 17/2 and human SaOS-2 cells. Biochem Biophys Res Commun 266: 448–453
11. **McAllister TN, Frangos JA** 1999 Steady and transient fluid shear stress stimulate NO release in osteoblasts through distinct biochemical pathways. J Bone Miner Res 14:930–936
12. **Fernandes AJ, Lora M, Patry C, Morisset S, Sarrazin P, Maciel F** 1997 Parathyroid hormone induction of cyclooxygenase-2 expression in human osteoblasts depends on both cyclic AMP and calcium-dependent pathways. Adv Exp Med Biol 433:303–306
13. **Klein-Nulend J, Semeins CM, Burger EH** 1996 Prostaglandin mediated modulation of transforming growth factor-β metabolism in primary mouse osteoblastic cells in vitro. J Cell Physiol 168:1–7
14. **Chambers TJ, Fox S, Jagger CJ, Lean JM, Chow JW** 1999 The role of prostaglandins and nitric oxide in the response of bone to mechanical forces. Osteoarthritis Cartilage 7:422–423
15. **Turner CH, Takano Y, Owan I, Murrell GA** 1996 Nitric oxide inhibitor L-NAME suppresses mechanically induced bone formation in rats. Am J Physiol 270:E634–E639
16. **Forwood MR** 1996 Inducible cyclo-oxygenase (COX-2) mediates the induction of bone formation by mechanical loading in vivo. J Bone Miner Res 11:1688–1693
17. **Li J, Burr DB, Turner CH** 2002 Suppression of Prostaglandin synthesis with NS-398 has different effects on endocortical and periosteal bone formation induced by mechanical loading. Calcif Tissue Int 70:320–329
18. **Ryder KD, Duncan RL** 2000 Parathyroid hormone modulates the response of osteoblast-like cells to mechanical stimulation. Calcif Tissue Int 67:241–246
19. **Ryder KD, Duncan RL** 2001 Parathyroid hormone enhances fluid shear-induced $[Ca^{2+}]_i$ signaling in osteoblastic cells through activation of mechanosensitive and voltage-sensitive Ca^{2+} channels. J Bone Miner Res 16:240–248
20. **Li J, Duncan RL, Burr DB, Turner CH** 2002 L-type calcium channels mediate mechanically induced bone formation in vivo. J Bone Miner Res 17:1795–1800
21. **Grundy JS, Eliot LA, Foster RT** 1997 Extrahepatic first-pass metabolism of nifedipine in the rat. Biopharm Drug Dispos 18:509–522
22. **McTavish D, Sorkin EM** 1989 Verapamil. An updated review of its pharmacodynamic and pharmacokinetic properties, and therapeutic use in hypertension. Drugs 38:19–76
23. **Fox J, Miller MA, Stroup GB, Nemeth EF, Miller SC** 1997 Plasma levels of parathyroid hormone that induce anabolic effects in bone of ovariectomized rats can be achieved by stimulation of endogenous hormone secretion. Bone 21:163–169
24. **Forwood MR, Bennett MB, Blowers AR, Nadorfi RL** 1998 Modification of the in vivo four-point loading model for studying mechanically induced bone adaptation. Bone 23:307–310
25. **Turner CH, Forwood MR, Rho JY, Yoshikawa T** 1994 Mechanical loading thresholds for lamellar and woven bone formation. J Bone Miner Res 9:87–97
26. **Torrance AG, Mosley JR, Suswillo RF, Lanyon LE** 1994 Noninvasive loading of the rat ulna in vivo induces a strain-related modeling response uncomplicated by trauma or periostal pressure. Calcif Tissue Int 54:241–247
27. **Hsieh YF, Wang T, Turner CH** 1999 Viscoelastic response of the rat loading model: implications for studies of strain-adaptive bone formation. Bone 25: 379–382
28. **Turner CH, Owan I, Alvey T, Hulman J, Hock JM** 1998 Recruitment and proliferative responses of osteoblasts after mechanical loading in vivo determined using sustained-release bromodeoxyuridine. Bone 22:463–469
29. **Hsieh YF, Robling AG, Ambrosius WT, Burr DB, Turner CH** 2001 Mechanical loading of diaphyseal bone in vivo: the strain threshold for an osteogenic response varies with location. J Bone Miner Res 16:2291–2297
30. **Pocotte SL, Ehrenstein G, Fitzpatrick LA** 1995 Role of calcium channels in parathyroid hormone secretion. Bone 16:365S–372S
31. **Bogin E, Chagnac A, Juppner H, Levi J** 1987 Effect of verapamil on plasma parathyroid hormone. J Clin Chem Clin Biochem 25:83–85
32. **Miyauchi A, Notoya K, Mikuni-Takagaki Y, Goto M, Miki Y, Takano-Yamamoto T, Jinnai K, Takahashi K, Kumegawa M, Chihara K, Fujita T** 2000 Parathyroid hormone-activated volume-sensitive calcium influx pathways in mechanically loaded osteocytes. J Biol Chem 275:3335–3342
33. **Walker LM, Publicover SJ, Preston MR, Said Ahmed MA, El Haj AJ** 2000 Calcium-channel activation and matrix protein upregulation in bone cells in response to mechanical strain. J Cell Biochem 79:648–661
34. **Caffrey JM, Farach-Carson MC** 1989 Vitamin D_3 metabolites modulate dihydropyridine-sensitive calcium currents in clonal rat osteosarcoma cells. J Biol Chem 264:20265–20274
35. **Fritsch J, Chesnoy-Marchais D** 1994 Dual modulation of the L-type calcium current of rat osteoblastic cells by parathyroid hormone: opposite effects of protein kinase C and cyclic nucleotides. Cell Signal 6:645–655
36. **Takeuchi K, Guggino SE** 1996 24R, 25-$(OH)_2$ vitamin D_3 inhibits 1α,25-$(OH)_2$ vitamin D_3 and testosterone potentiation of calcium channels in osteosarcoma cells. J Biol Chem 271:33335–33343
37. **Yukihiro S, Posner GH, Guggino SE** 1994 Vitamin D_3 analogs stimulate calcium currents in rat osteosarcoma cells. J Biol Chem 269:23889–23893
38. **Li W, Duncan RL, Karin NJ, Farach-Carson MC** 1997 1,25$(OH)_2D_3$ enhances PTH-induced Ca^{2+} transients in preosteoblasts by activating L-type Ca^{2+} channels. Am J Physiol 273:E599–E605
39. **Duncan RL, Hruska KA, Misler S** 1992 Parathyroid hormone activation of stretch-activated cation channels in osteosarcoma cells (UMR-106.01). FEBS Lett 307:219–223
40. **Yamaguchi DT, Hahn TJ, Iida-Klein A, Kleeman CR, Muallem S** 1987 Parathyroid hormone-activated calcium channels in an osteoblast-like clonal osteosarcoma cell line. cAMP-dependent and cAMP-independent calcium channels. J Biol Chem 262:7711–7718
41. **Guggino SE, Lajeunesse D, Wagner JA, Snyder SH** 1989 Bone remodeling signaled by a dihydropyridine- and phenylalkylamine-sensitive calcium channel. Proc Natl Acad Sci USA 86:2957–2960
42. **Valin A, Guillen C, Esbrit P** 2001 C-terminal parathyroid hormone-related protein (PTHrP) (107–139) stimulates intracellular Ca^{2+} through a receptor different from the type 1 PTH/PTHrP receptor in osteoblastic osteosarcoma UMR 106 cells. Endocrinology 142:2752–2759
43. **Duncan RL, Akanbi KA, Farach-Carson MC** 1998 Calcium signals and calcium channels in osteoblastic cells. Semin Nephrol 18:178–190
44. **Duriez J, Flautre B, Blary MC, Hardouin P** 1993 Effects of the calcium channel blocker nifedipine on epiphyseal growth plate and bone turnover: a study in rabbit. Calcif Tissue Int 52:120–124
45. **Dobnig H, Turner RT** 1995 Evidence that intermittent treatment with parathyroid hormone increases bone formation in adult rats by activation of bone lining cells. Endocrinology 136:3632–3638
46. **Hodsman AB, Steer BM** 1993 Early histomorphometric changes in response to parathyroid hormone therapy in osteoporosis: evidence for de novo bone formation on quiescent cancellous surfaces. Bone 14:523–527
47. **Jilka RL, Weinstein RS, Bellido T, Roberson P, Parfitt AM, Manolagas SC**

1999 Increased bone formation by prevention of osteoblast apoptosis with parathyroid hormone. J Clin Invest 104:439–446
48. **Juppner H, Abou-Samra AB, Freeman M, Kong XF, Schipani E, Richards J, Kolakowski Jr LF, Hock J, Potts Jr JT, Kronenberg HM, Segre GV** 1991 A G protein-linked receptor for parathyroid hormone and parathyroid hormone-related peptide. Science 254:1024–1026
49. **Swarthout JT, D'Alonzo RC, Selvamurugan N, Partridge NC** 2002 Parathyroid hormone-dependent signaling pathways regulating genes in bone cells. Gene 282:1–17
50. **Yamaguchi DT, Kleeman CR, Muallem S** 1987 Protein kinase C-activated calcium channel in the osteoblast-like clonal osteosarcoma cell line UMR-106. J Biol Chem 262:14967–14973
51. **Joborn H, Bergstrom R, Rastad J, Wide L, Akerstrom G, Ljunghall S** 1988 Effects of propranolol and verapamil on plasma ionized calcium and parathyroid hormone in short-term intense isokinetic leg exercise. Clin Physiol 8:1–7
52. **Wynne AG, Romanski SA, Klee GG, Ory SJ, O'Fallon WM, Fitzpatrick LA** 1995 Nifedipine, but not verapamil, acutely elevates parathyroid hormone levels in premenopausal women. Clin Endocrinol (Oxf) 42:9–15
53. **Ambudkar SV, Dey S, Hrycyna CA, Ramachandra M, Pastan I, Gottesman MM** 1999 Biochemical, cellular, and pharmacological aspects of the multidrug transporter. Annu Rev Pharmacol Toxicol 39:361–398
54. **Robling AG, Burr DB, Turner CH** 2000 Partitioning a daily mechanical stimulus into discrete loading bouts improves the osteogenic response to loading. J Bone Miner Res 15:1596–1602
55. **Robling AG, Duijvelaar KM, Geevers JV, Ohashi N, Turner CH** 2001 Modulation of appositional and longitudinal bone growth in the rat ulna by applied static and dynamic force. Bone 29:105–113